

MicroRNAs Align With Accessible Sites in Target mRNAs

Weihua Pan,¹ Ping Xin,¹ and Gary A. Clawson^{1,2*}

¹Departments of Pathology and Biochemistry & Molecular Biology, Gittlen Cancer Research Foundation, Hershey Medical Center, Pennsylvania State University, Hershey, Pennsylvania

²Materials Research Institute, Pennsylvania State University, State College, Pennsylvania

ABSTRACT

The importance of microRNAs (miRs) in control of gene expression is now clearly recognized. While individual microRNAs are thought to target hundreds of disparate mRNAs via imperfect base pairing, little is known about the characteristics of miR target sites. Here we show that the miRs can be aligned with empirically identified accessible sites in a target RNA (Cytokeratin 19, KRT), and that some of the aligned miRs functionally down-regulate KRT expression post-transcriptionally. We employed an RNase-H-based random library selection protocol to identify accessible sites in KRT RNA. We then aligned the Sanger Institute database collection of human miRs to KRT mRNA, and also aligned them using the web-based MicroInspector program. Most miRs aligned with the accessible sites identified empirically; those not aligned with the empirically identified sites also functioned effectively in RNase-H-based assays. Similar results were obtained with a second target RNA (Mammoglobin). Transient transfection assays established that some of the miRs which aligned with KRT significantly down-regulated it at the protein level, with no effect on RNA level. The functionally effective miRs aligned within the coding region of KRT, whereas a number of miRs which aligned with the 3'-untranslated region did not produce down-regulation. *J. Cell. Biochem.* 109: 509–518, 2010. © 2009 Wiley-Liss, Inc.

KEY WORDS: microRNAs; LIBRARY SELECTION

Understanding of mechanisms controlling gene expression has been rapidly changing with the discovery of small non-coding RNA molecules, termed microRNAs (miRs) [Bartel, 2004; Wu and Belasco, 2008]. Several hundred miRs are already included in the Wellcome Sanger Institute database, with many more being added weekly. miRs are thought to target a significant portion of the entire population of all mRNAs, and due to generally imperfect sequence matches with target RNAs, each miR may actually target 100–200 different mRNAs [Bushati and Cohen, 2007; Nilsen, 2007], suggesting complex wide-ranging effects. miRs can even act as oncogenes [Esquela-Kerscher and Slack, 2006] or as tumor suppressors [Zhang et al., 2007], and the importance of miRs in many (if not all) cancers is becoming clear [Calin et al., 2005; Iorio et al., 2005; Lu et al., 2005; Kluiver et al., 2006; Volinia et al., 2006; Ambs et al., 2008]. In spite of their rapid discovery and ongoing experimental validation, *why* miRs are directed to particular sites in target RNAs remains mysterious. Here we employ an RNase-H-based random library selection protocol [Pan and Clawson, 2006] to identify accessible sites in a selected target mRNA (Cytokeratin 19, KRT). We then aligned the Sanger Institute database collection of

human miRs to KRT mRNA (using two methods) and identified a considerable number of miRs which could be aligned. Most miRs aligned with the accessible sites identified empirically; those not aligned with the empirically identified sites also functioned effectively in RNase-H-based assays. Analogous results were observed with a second target RNA (mammoglobin, MGB). Some of the miRs which aligned with KRT significantly down-regulated it at the protein level, with no effect on RNA level. Functionally effective miRs aligned within the coding region of KRT, whereas a number of miRs which aligned with a prominent site in the 3'-untranslated region did not produce down-regulation.

MATERIALS AND METHODS

TARGET RNA PREPARATION AND N17 LIBRARY SELECTION

Reverse transcription/PCR (RT-PCR) was used to generate the pre-template construct (no promoter) of KRT (1,466 nucleotides (nt) in length, gi: 40217850). This was performed using total RNA isolated from MCF7 cells (human mammary adenocarcinoma, ATCC BHT-22TM) for KRT, using TRIzol Reagent (Gibco BRL). The RT-PCR

Additional Supporting Information may be found in the online version of this article.

Grant sponsor: NIH/NCI IMAT; Grant number: CA118591; Grant sponsor: Gittlen Cancer Research Foundation.

*Correspondence to: Dr. Gary A. Clawson, PhD, MD, Director, Gittlen Cancer Research Foundation, H059, Hershey Medical Center, Pennsylvania State University, 500 University Drive, Hershey, PA 17033. E-mail: gac4@psu.edu

Received 13 July 2009; Accepted 22 October 2009 • DOI 10.1002/jcb.22428 • © 2009 Wiley-Liss, Inc.

Published online 8 December 2009 in Wiley InterScience (www.interscience.wiley.com).

products were generated using primer pairs of 5'-CGC CCC TGA CAC CAT T-3' and 5'-TTT CCC TTG GAC CATA-3' for KRT as previously described [Pan et al., 2003]. Products were cloned into PCR2.1-TOPO vector (Invitrogen) and were sequenced in their entirety prior to use. Double-stranded DNA templates for production of target RNA transcripts were constructed by adding the T7 RNA polymerase promoter along with the further PCR amplification by primer pairs: For KRT₃₆₆₋₁₀₆₇ (nt 366-1067), the primers were 5'-CCG AAG CTT AAT ACG ACT CAC TAT AGG GCA ACG AGA AGC TAA CCA T-3' and 5'-TGC AGC TCA ATC TCA AGA C-3'. For KRT₉₆₇₋₁₄₆₆ (nt 967-1466, a transcript which included the 3'-untranslated region of KRT), the primers were 5'-CCG AAG CTT AAT ACG ACT CAC TAT AGG GTT GAA CCG GGA GGT CGC TGG and 5'-TTT CCC TTG GAC CATA. Constructs were again sequenced prior to use.

The target KRT₃₆₆₋₁₀₆₇ and KRT₉₆₇₋₁₄₆₆ RNA transcripts were transcribed *in vitro* using the Riboprobe System (Promega) by T7 RNA polymerase, followed by an RNase-free DNase digestion to destroy the template DNAs, and RNA transcripts were purified by PAGE [Pan et al., 2004]. To produce 5'-end (³²P)-labeled target RNAs, an alkaline phosphatase (Calf Intestinal, New England Biolabs) was employed to remove tri-phosphate group from 5'-end of the transcripts, and the transcripts were then labeled using T4 polynucleotide kinase (New England Biolabs) with γ -(³²P)-ATP and transcripts were again purified by PAGE [Pan and Clawson, 2004].

For the N₁₇-RNase-H selection procedure [Pan and Clawson, 2006]: (i) a trace amount (100K cpm) of 5'-end (³²P)-labeled target RNA in 2 μ l of 20 mM Tris-HCl (pH 7.4) was chilled on ice for 3 min, and 1 μ l of 50 mM MgCl₂ was added, and the sample was heated for 3 min at 85°C; (ii) sample was incubated 3 min at 37°C, and then 1 μ l of 100 μ M N₁₇ (5'-NNN NNN NNN NNN NN-3') random library was added (or 20 mM Tris-HCl as a control) and incubated 10 min at 37°C; (iii) 1 μ l of 1 U/ μ l RNase-H (Ambion) was added, and sample was incubated 15 min at 37°C. Seven microliters of 2 \times RNA loading buffer was then added. A/G and limited alkaline hydrolysis (H) ladders were also prepared as described [Pan and Clawson, 2004], and the samples were analyzed by PAGE using 6% urea sequencing gels running 1.5, 4, and finally 7.5 h at 56 W. The gels were dried and then exposed to autoradiographic film.

These same procedures were also used for the coding region of human mammoglobin (MGB₁₋₅₀₂, gi: 142378579), which was amplified from human breast tissue specimens. The primers used for the initial amplification of the MGB₁₋₅₀₂ region were 5'-GAC GCG GCT TCC TTG-3'/5'-TGC CAT CAA TTT ATT AAA ATA AAC AT-3'.

mFold plots of the two KRT segments, and the MGB segment, are included as Supplementary Online Material, with the library-selected regions marked. In general, library-selected regions span junctions between single-stranded loops and double-stranded regions, although not all such regions in the target RNAs are identified as accessible.

MacVECTOR™ miR-LIBRARY CONSTRUCTION AND TARGET RNA ALIGNMENTS

The human mature miR sequences were downloaded from the Sanger Institute website <http://microrna.sanger.ac.uk> [Griffiths-Jones et al., 2007], and a MacVector™ miR-Library containing 730

miRs with an average size of 22 nt in length was constructed. Each miR was then aligned individually with the KRT₃₆₆₋₁₀₆₇ and KRT₉₆₇₋₁₄₆₆ sequences. We then selected miRs with match scores of ≥ 44 , which was greater or equal to half of the maximum score (88) for a 22-nt sequence. The MacVector alignment results for KRT₃₆₆₋₁₀₆₇ and KRT₉₆₇₋₁₄₆₆ sequences are shown in Tables I and II, respectively. The same procedures were used to construct a library and alignment for human MGB₁₋₅₀₂ sequences.

As an alternative method, we also used the web-based MicroInspector tool [Rusinov et al., 2005] to identify potential miR targeting sites within the KRT RNA sequences, as well as for miR sites within the MGB₁₋₅₀₂ sequence. The tool can be accessed at <http://bioinfo.uni-plovdiv.bg/microinspector>.

Overlap was considered to exist if ≥ 5 nt from the MiR overlapped the minimal (17 nt) accessible site defined empirically.

ANALYSIS AND COMPARISON

Antisense oligonucleotides (ASO) against the identified miR target sites were synthesized, and ASO-RNase-H cleavage reactions were performed in the same manner as the N17 library selections, but with the specific ASO diluted from a concentration of 200 nM as a standard test (or 20 μ M for a high concentration comparison). After incubations, samples were separated by PAGE in a urea-polyacrylamide gel, and the gels were then dried and radioactivity was analyzed using a Phosphor-Imager as previously described.

For transient transfection assays, miRs were synthesized which contained all 2'-O-methyl substitutions (from Integrated DNA Technologies), which targeted various regions within KRT₉₆₇₋₁₄₆₆. These included: (A) miR-125b-1 and miR-615-59, two miRs which aligned with R1 in the coding region; (B) miR-138, which aligned between R2 and R3; (C) miR-let-7b, which aligned with R6; and (D) miR-205, miR-150, and miR-211, all of which aligned with R7 within the 3'-untranslated region of KRT. We also tested three miRs which aligned with lower MacVector match scores (34-38) to KRT; these included miR-let-7c*, miR-let-7f, and miR-let-7g. Two random miRs were also synthesized.

MCF7 cells were transfected with the designated miRs (10 μ l of 20 mM miR + 3 μ l oligofectamine/well on 6-well plates). Negative controls included transfections without miR, and no transfection procedure, as well as a random miR which did not align with KRT (the random sequence AUCGAAUCCAAGUGCCUAGAUC was used in some experiments). Forty-eight hours following transfections, cells were harvested for RNA and protein isolations using Trizol (Invitrogen) and lysis buffer reagents (respectively), according to manufacturer's recommendations. Three independent experiments were performed in triplicate.

RNA preparations were treated with Turbo DNA-free reagent (Ambion), and 100 ng aliquots were used in QPCR reactions, which were performed as described [Pan et al., 2003], using TaqMan methodology and a Stratagene 4000X. For KRT₅₄₈₋₆₄₈, the forward primer was 5'-GGGACAAGATTCTTGGTGCC, reverse primer was 5'-CGTCTCAAACCTTGTTTCGGAA, and the fluorogenic probe was 5'-FAM-CCATTGAGAACTCCAGGATTGTCTGCA-BHQ1. Tata-box-binding protein was used as the internal standard as described [Pan et al., 2003], using a CAL-fluor Orange 560-labeled fluorogenic probe. In follow-up studies, we also amplified KRT₁₂₈₁₋₁₃₈₁ using the

primer-probe set: forward primer: 5'-CCTGCTCGAGGGACAGGAA; reverse primer: 5'-AGACACCCTCCAAAGGACAGC; and TaqMan probe: Cy5 5'd-Quasar670-CTGCCTCCAAGGTCCTCTGAGGCA-BHQ-2.

Further examinations of KRT RNA levels were also performed by Northern blot analysis as previously described [Pan et al., 2004, #3015] using 5 µg of total RNA and KRT₃₆₇₋₁₀₆₆ and KRT₉₆₇₋₁₄₆₆ probes labeled by random priming.

TABLE I. KRT₃₆₆₋₁₀₆₇-mRNA/miR-Library (MacVector™ 8.0) Search Results

miRNA	nt	Max Score	KRT Score	Location	Alignment
let-7i	22	88	44	528-515	KRT <GTAGTA G--TG-GCTG T let7i GTAGTA GTTTGTGCTG T KRT <GCCGAC CTTGTCCAGG TAG miR-18a GTGCAT CTAGTGCAGA TAG KRT <AGTTCTCAAT GGTGGCACCA miR-19a* AGTTTTGCAT AGTTGCACTA KRT <GCCGAC CTTGTCCAGG TAG miR-20b GTGCTC ATAGTGCAGG TAG KRT <CGGGAGGGCC CAGGCCCTG miR-149* AGGGAGGGAC GGGGGCTGTG KRT <GTTCTCAATG GTGGCA-CC miR-182 TTTGGCAATG GTAGAACTC KRT <GAT-CTGCAG GACAATCCTG G miR-200a* CATCTTACCG GACAGTGTG G KRT <AT-CTGCA GGACAATCCT GGA miR-200c ATACTGCC GGGTAATGAT GGA KRT <ATGGTCGTGT AGTAGTGGCT miR-210 CTGTGCGTGT GACAGCGGCT KRT <GC-G-CACCT TGTCCAGG miR-345 GCTGACTCCT AGTCCAGG KRT <ATCTGCAT CTCCAGG miR-361-5p ATCAGAAT CTCCAGG KRT <GCCTCCAGGG CGCGCACCTT GT miR-370 GCCTGCTGGG GTGGAACTG GT KRT <AG-CCAGACG GGCATTGTGCG AT miR-383 AGATCAGAAG GTGATTGTGG CT KRT <CAGCTCTTCC TTCAGGCCTT C miR-431* CAGGTCGTCT TGCAGGGCTT C KRT <TGGTCGTGTA GTAGTGGCTG miR-449a TGGCAGTGTG TTGTTAGCTG KRT <AACTCTGGAG TTCTCAATGG T miR-490-3p CAACCTGGAG GACTCCATGC T KRT <TGCATCT CCAGGTCGGT miR-490-5p TGGATCT CCAGGTGGGT KRT <TCA-TGGTTC TTCTCAGGT AG miR-509-3p TGATTGGTAC GTCTGTGGGT AG KRT <GTTCTGCATG GTTAG miR-544 ATTCTGCAT TTAG KRT <CCGTCTCAA CTTG-GTTTCG miR-551b GCGACCCATA CTGGTTTCA KRT <TACCAG TCGCGGATCT T miR-556-3p TACCAT TAGCTCATCT T KRT <GCTCGC CGTTGGCC miR-572 GCTCGC CGTTGGCC KRT <CACGCTCATG CGCAGAGCC

(Continued)

TABLE I. (Continued)

miR-624*	22	88	46	485-464	miR-574-3p KRT	 CACGTCATG CACACACC <TGGTACCAGT CGCGGATCTT CA
miR-628-3p	21	84	44	532-513	miR-624* KRT	 TAGTACCAGT ACCTTGTGT CA <TCGTGTAGTA GTGGCTGTAG
miR-640	21	84	48	505-485	miR-628-3p KRT	 TCTAGTAAGA GTGGCAGTCG <AGGGCCAGG CCCCTGCTTC T
miR-708	23	92	44	472-453	miR-640 KRT	 ATGATCCAGG AACCTGCCCTC T <GGATCTTC ACCTCTAGCT CG
miR-886-5p	23	92	44	725-703	miR-708 KRT	 GGAGCTTA CAATCTAGCT GG <CTGGCCAGG TCAGCTCATC CAG
miR-936	22	88	44	526-507	miR-886-5p KRT	 CGGTCGGAG TTAGCTCAAG CGG <AGTAGTGG CTGTAGTCGC GG
miR-943	21	84	48	456-436	miR-936 KRT	 AGTAGAGG GAGGAATCGC AG <CTCGCCGTTG GCCGCCTCCA G
miR-1225-3p	22	88	50	453-436	miR-943 KRT	 CTGACTGTTG CCGTCTCCA G <GCCGTTG -GCCGCCTCC AG
					miR-1225-3p	 GCCCTG TGCCGCCCC AG

Immunoblot analyses were performed as described [Clawson et al., 2008], using an anti-KRT (CK19) rabbit polyclonal antibody (Novus Biologicals) at 1:10,000 dilution, with a goat anti-rabbit secondary antibody. After staining, the blots were stripped using a Western Blot Recycling kit (Alpha Diagnostic International), and re-probed using a β -actin antibody (Cell Signaling) at 1:5,000 dilution. Controls included no primary antibody.

RESULTS AND DISCUSSION

We selected KRT as a representative target RNA for miRs. We performed library selection on segments encompassing the coding region (KRT₃₆₆₋₁₀₆₇) and a segment also containing the 3'-untranslated region (KRT₉₆₇₋₁₄₆₆) of KRT RNA, using a random N17 library and an RNase-H digestion protocol [Pan and Clawson, 2006]. The random library DNA (17 nt) hybridizes to accessible sites on the RNA, promoting degradation of those sites by RNase-H, and allowing identification of the sites on sequencing gels (by comparison with limited hydrolysis ladders). The library selection identified 12 accessible regions for the KRT₃₆₆₋₁₀₆₇ RNA and 7 accessible regions in KRT₉₆₇₋₁₄₆₆ (see Fig. 1A).

Next, the collection of human mature miRs was downloaded from the Wellcome Sanger Institute database [Griffiths-Jones et al., 2007] and a MacVector™ miR-Library containing 730 human miRs with an average size of 22 nt in length was constructed. The miRs in the library were then matched individually against the KRT₃₆₆₋₁₀₆₇ transcript, and 32 complementary miRs could be aligned with KRT₃₆₆₋₁₀₆₇ RNA with match scores of at least 44 (half of the maximum score; see Table I). Using the MacVector library about 75% of the complementary miRs for KRT₃₆₆₋₁₀₆₇ RNA overlapped with regions identified by the empirical library selection protocol (Table I). None of these miRs has been identified as targeting KRT. Intriguingly, three miRs aligned (with scores ≥ 44) with KRT₃₆₆₋₁₀₆₇ in the "sense" orientation. For example, miR-412 aligned with a

match score of 52 (with a segment of it matching a stretch of 14 of 16 nucleotides in KRT₃₆₆₋₁₀₆₇).

Using the web-based MicroInspector tool [Rusinov et al., 2005], 80% of all the miRs which aligned to KRT₃₆₆₋₁₀₆₇ overlapped (≥ 5 nt) accessible regions identified by library selection (Fig. 2A). One region in KRT₃₆₆₋₁₀₆₇, designated R9, had 17 miRs that overlapped it.

ASOs (17mers, equivalent in size to the ASOs used in the random library selection protocols) were synthesized corresponding to regions 1-8 in the KRT₃₆₆₋₁₀₆₇ library selection, and they were then tested in the corresponding ASO-RNase-H cleavage reactions. For KRT₃₆₆₋₁₀₆₇, average cleavage was $38.3 \pm 8.4\%$ of target (not shown; see below). With higher concentrations of ASO, we also observed multiple cleavage sites for some of the regions (not shown). We also arbitrarily chose three ASOs that were *not* located within accessible, library-selected sites (clear regions on the sequencing gels). Use of these ASOs resulted in very low cleavage rates in the RNase-H-based assay (Fig. 1C, designated as N1-3; cleavage was $2.1 \pm 0.6\%$).

For KRT₉₆₇₋₁₄₆₆, library selection identified seven accessible regions (Fig. 1A). Using the MacVector approach, 33 miRs could be aligned with KRT₉₆₇₋₁₄₆₆, and the percentage of miRs which aligned with accessible regions was 76% (see Table II). When the ASOs corresponding to regions 1-7 were synthesized and tested in RNase-H-based cleavage assays, most (5 of 7) of them showed very good activity in ASO-RNase-H reactions (Fig. 1B), and ASO targeted to other regions within KRT₉₆₇₋₁₄₆₆ to which miRs aligned also showed good activity (not shown). The library-selected region R7 which showed the most overlapping aligned miRs (Fig. 2B) lies within the 3'-untranslated region (see also below). For this site, two of the miRs which aligned with the KRT₉₆₇₋₁₄₆₆ target were in the sense orientation.

As noted, ASOs targeted to sites R1 and R7 of KRT₉₆₇₋₁₄₆₆ showed only weak cleavage activity (Fig. 1B). Since we have not observed poor activity of selected ASOs before with any of our other selection protocols [Pan et al., 2001, 2003; Pan and Clawson, 2004; Pan and Clawson, 2006], we re-performed the protocols and in addition also

examined the RNase-H digestion sequencing gels in more detail. We found RNase-H was actually initiating hydrolysis 5–9 nucleotides upstream from the 3'-end of the ASO/target RNA match, rather than at the 3'-end. All of the ASOs were therefore correspondingly shifted

by six nucleotides in the target RNA sequences and cleavage was retested. For the shifted ASO targeting regions R1 and R7 (designated as Δ1 and Δ7), both showed major increases in activity; Δ1 was 5× more active, and Δ7 was ~4× more active than the

TABLE II. KRT₉₆₇₋₁₄₆₆-mRNA/miR-Library (MacVector™ 8.0) Search Results

miRNA	nt	Max Score	KRT Score	Location	Alignment
let-7i*	22	88	44	1260-1240	KRT <CTGCTCCAGC CGC-GACTTG AT let-7i* CTGCGCAAGC TACTGCCTTG CT KRT <TGG-AGGC-A GACAAATTGT TGT miR-7 TGGAAAGACTA GTGATTTTGT TGT KRT <CCAGAG CCTGCTGCCT CA miR-15a* CCATAT TGTGCTGCCT CA KRT <AGGCTGCGGT AGGTGGCAAT -CT miR-92a-1* AGGTTGGGAT CGGTTGCAAT GCT KRT <ACT-ATCAGC TCGCACATCG C miR-93* ACTGCTGAGC TAGCACTTCC C KRT <TCCCTTGGAC CATAAATTTT TA miR-125b TCCCTGAGAC CCTAACTTGT GA KRT <TGCCTC AGAGGACCTT G miR-148b TGCAATC ACAGAACTTT G KRT <ACCATAAATT TTTATTGGCA GGT miR-181d AACATTCAAT GTTGTGCGGT GGT KRT <TGCTGCCTCA GAGGACCTTG miR-187* GGCTACAACA CAGGACCCGG KRT <CAGCAGAAGC CCCAGAGC-- CTG miR-191 CAACGGAATC CAAAAGCAG CTG KRT <TCAGCGCCTG GATA-T-GCG C miR-191* GCTGCGCTTG GATTTCGTCC C KRT <TGTGACTGCA GCTCAATCT miR-194 TGTAACAGCA ACTCCATGT KRT <TCTTCCAA GGCAGCTTF miR-200b* TCTTACTG GGCAGCATT KRT <GCGCCTCCGT TTCTGCCAG miR-220b CCACCACCGT GTCTGACAC KRT <GCCCCAG AGCCTGCTG miR-324-3p GCCCCAG GTGCTGCTG KRT <GTCCCTTC CTCCCATCC CT miR-328 GGCCCTCT CTGCCCTTCC GT KRT <TTTCTGCCAG TGTGCTTCC miR-346 TGTCTGCCCG CATGCCTGCC KRT <TCGCCAGCT GGGCTC-AA T miR-361-3p TCCCCAGGT GTGATTCTGA T KRT <AGCTCAATCT CAAGACCCTG A miR-423-3p AGCTCGGTCT GAGGCCCTC A KRT <CTCATCTGGA GCTGCTCCGT G miR-433 ATCATGATGG GCTCCTCGGT G KRT <GGCAGGT CAGGAGAAGA miR-486-3p GGCAGCT CAGTACAGGA KRT <CTGCGGTA GGTGGCAATC miR-509-5p CTGCAGAC AGTGGCAATC KRT <CTCCAAG GACAGCA

(Continued)

TABLE II. (Continued)

miR-545*	22	88	48	1455-1440	miR-515-5p KRT	 CTCCAAA GAAAGCA <CC-ATAAATT TTTATTG
miR-567	23	92	54	1106-1088	miR-545* KRT	TCAGTAAATG TTTATTA <AGTGTG-TCT TCCAAGGCAG
miR-637	24	96	46	1092-1074	miR-567 KRT	AGTATGTCT TCCAGGACAG <GGCAGCT TTCATGCTCA GC
miR-642	22	88	46	1112-1097	miR-637 KRT	GGGGGCT TTCGGGCTCT GC <TCTGC CAGTGTGTCT T
miR-645	19	76	50	1228-1215	miR-642 KRT	TCTCC AAATGTGTCT T <GCTGG TACTCCTGA
miR-654-5p	22	88	50	1042-1025	miR-645 KRT	GCTGG TACTCCTGA <GGGTGCGCCG CAGGTC-AG
miR-766	22	88	46	1357-1345	miR-654-5p KRT	TGGTGGGCG CAGAACATG <AGCCC CAGAGCCT
miR-873	21	84	44	1228-1209	miR-766 KRT	AGCCC CACAGCCT <GCTGGTACTC CTGATTCTGC
miR-885-5p	22	88	44	1409-1389	miR-873 KRT	GCAGGAAGT GTGAGTCTCC <TCCCTT-CCT TCCCATCCCT CT
miR-1227	20	80	44	1124-1105	miR-885-5p KRT	TCCATTACAC TACCCTGCCT CT <CGCGCCTCCG TTTCTGCCAG
					miR-1227	CGTGCCACCC TTTTCCCAG

original ASOs (Fig. 1B). The other five shifted ASOs showed activity, which was comparable to that shown by their unshifted counterparts ($100 \pm 14\%$), thus suggesting that some sites have more stringent constraints than others. This is of particular interest with $\Delta 7$, since it suggests that the accessible site may actually encompass all 12 of the miRs which aligned with region R7 in KRT₉₆₇₋₁₄₆₆ using the MicroInspector program (Fig. 2B; seven overlapped and five were located immediately 3' to the 17-nt site). Using the shifted results, cleavage for the library-selected ASOs was $30.5 \pm 7.6\%$ (Fig. 1B), similar to the cleavage rate for library-selected sites in KRT₃₆₆₋₁₀₆₇.

For comparison, we also performed a library selection on a portion of human mammoglobin (MGB₁₋₅₀₂) and repeated the alignment procedures with the MacVector miR library and the microInspector program. Eight accessible regions were identified in MGB₁₋₅₀₂ (Fig. 3). Testing of the corresponding ASOs in RNase-H-based assays showed cleavage rates of $36.3 \pm 2.9\%$ (Fig. 3C; shifted versions produced similar results for all sites). Fifty-two complementary miRs could be aligned with MGB₁₋₅₀₂ RNA, with match scores of ≥ 44 with the MacVector library, and 2/3 of them overlapped with the accessible sites. With the MicroInspector tool, 36 miRs aligned with MGB₁₋₅₀₂, and $\sim 86\%$ of them overlapped (≥ 5 nt) the library-selected accessible sites.

We also arbitrarily selected three miRs (Fig. 3) that aligned to three different regions in the MGB₁₋₅₀₂ transcript (miR-675, miR-770-5p, and miR-593, which aligned with library-selected regions R2, R3, and R6, respectively). Using 17mer ASOs representing the regions of these miR sequences which showed the best homology to the MGB target (designated as S1-3; see Fig. 3B,D for the sequence and alignment of the S1 ASO), we then tested them in ASO-RNase-H cleavage reactions, in comparison with a 17mer ASO matching the

R6 region (Fig. 3E). As expected, the ASO targeting R6 showed good activity, and all three ASOs from the miR aligned sequences (designated as S1-3) also showed good cleavage activity (Fig. 3E; cleavage was $26.8 \pm 6.6\%$, which did not differ from the library-selected ASO cleavage), indicating that the sites were readily accessible.

Further testing was next performed with the KRT constructs. We made ASOs restricted to the 5' 17-nt of the potential target sites (the so-called "seed regions") for three representative miRs (miR-205, miR-150, and miR-211) which aligned with region 7 in KRT₉₆₇₋₁₄₆₆. All of these ASOs functioned with intermediate effectiveness in the RNase-H-based assays (not shown), producing cleavage rates of $17.8 \pm 1.6\%$ ($P \leq 0.001$ vs. non-selected sites with $2.1 \pm 0.6\%$ cleavage).

Finally, for testing in cell culture, we synthesized a number of miRs which contained 2'-O-methyl modified ribonucleotides. These included: (A) two miRs which aligned with R1 in the coding region of the KRT₉₆₇₋₁₄₆₆ transcript (miR-125b-1 and miR-615-5p), another miR which aligned between R2 and R3 (miR-138), and an miR which aligned with R6 (miR-let-7b); and (B) three miRs which aligned with R7 from within the untranslated region of KRT₉₆₇₋₁₄₆₆ (miR-205, miR-150, and miR-211); and (C) three additional miRs which aligned with KRT₉₆₇₋₁₄₆₆ with lower MacVector match scores (34-38; these were let-7c*, let-7f, and let-7g). These were used in transient transfection assays with MCF7 cells, with RNA and protein harvested after 48 h. QPCR analyses showed that transfections with any of these miRs did not affect KRT mRNA levels in the cells (Fig. 2C; random miRs were also without effect). These results were further corroborated by QPCR analyses with an additional KRT amplicon, as well as Northern blot analyses, which also showed no change in KRT mRNA levels (Fig. 4).

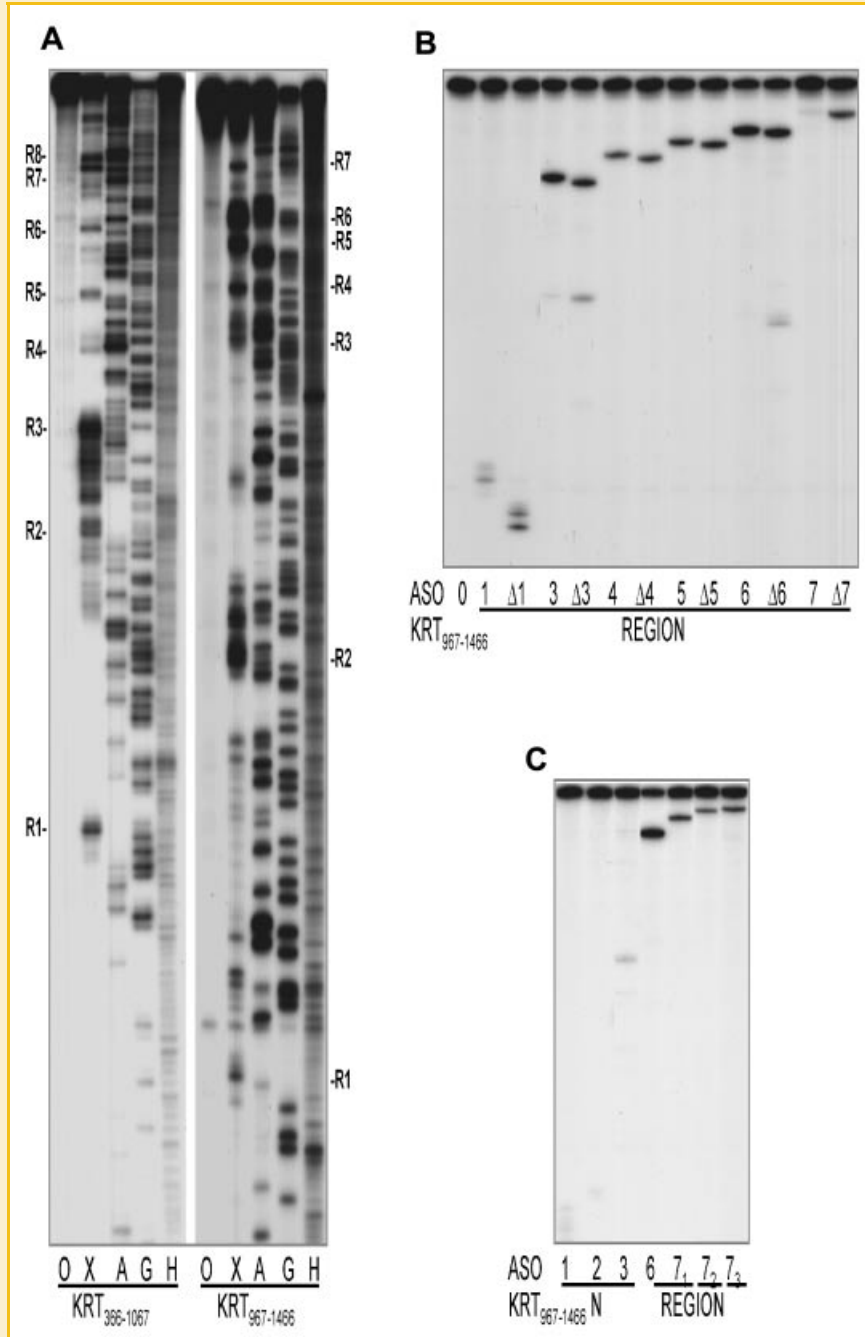


Fig. 1. N17 random library selection of accessible sites in KRT₃₆₆₋₁₀₆₇ and KRT₉₆₇₋₁₄₆₆ transcripts. An N17-RNase-H library selection was performed and the results analyzed on sequencing gels (panel A). Lanes show: O = control (no RNase-H); X = experimental; A = limited hydrolysis with RNase-U2, which cleaves at A residues; G = limited hydrolysis with RNase-T1, which cleaves at G residues; and H = limited base hydrolysis, which cleaves randomly at all residues. In the KRT₃₆₆₋₁₀₆₇ selection (left panel in A), 12 "regions" (R1-12) were identified. Regions are shown as encompassing 17 nt, but the accessible regions may extend in either direction. Regions 1-8 were identified on sequencing gels run for 1.5 h (shown in A); four additional regions, R9-12, were identified on sequencing gels run for 7.5 h (not shown). ASO targeted to the R1-8 regions were then synthesized and tested in specific ASO-RNase-H cleavage reactions. Another N17-RNase-H library selection was performed on KRT₉₆₇₋₁₄₆₆ (right panel of A), a transcript which also contained the 3'-untranslated region, and seven regions were identified (R1-7). Specific ASO 17mers were synthesized which corresponded to these regions, and tested under the same selection procedure (panel B). Surprisingly, only five of the seven ASOs produced good RNase-H cleavage activity (the ASO targeting R1 and R7 showed very weak activities). When we re-performed and re-examined sequencing gels from the RNase-H-based selections, we found that RNase-H was actually initiating hydrolysis 5-9 nt from the 3'-end of the ASO regions. We re-synthesized ASO targeting regions R1 and R7 which were correspondingly shifted by six nucleotides (designated as $\Delta 1$ and $\Delta 7$), as well as shifted version for the other regions. When RNase-H protocols were re-performed with the $\Delta 1$ and $\Delta 7$ ASOs, cleavage was substantially increased for both regions (panel B), yielding results equivalent to those obtain for the other regions. Panel C shows RNase-H-based cleavage results with three ASOs to regions which did not show any activity in library selection protocols (N1-N3), as well as cleavage of three ASOs matching particular sequences to which three miRs aligned within region 7 (miR-205, miR-150, and miR-211, designated as 7₁-7₃). ASOs targeting the library-selected R6 region is shown for comparison.

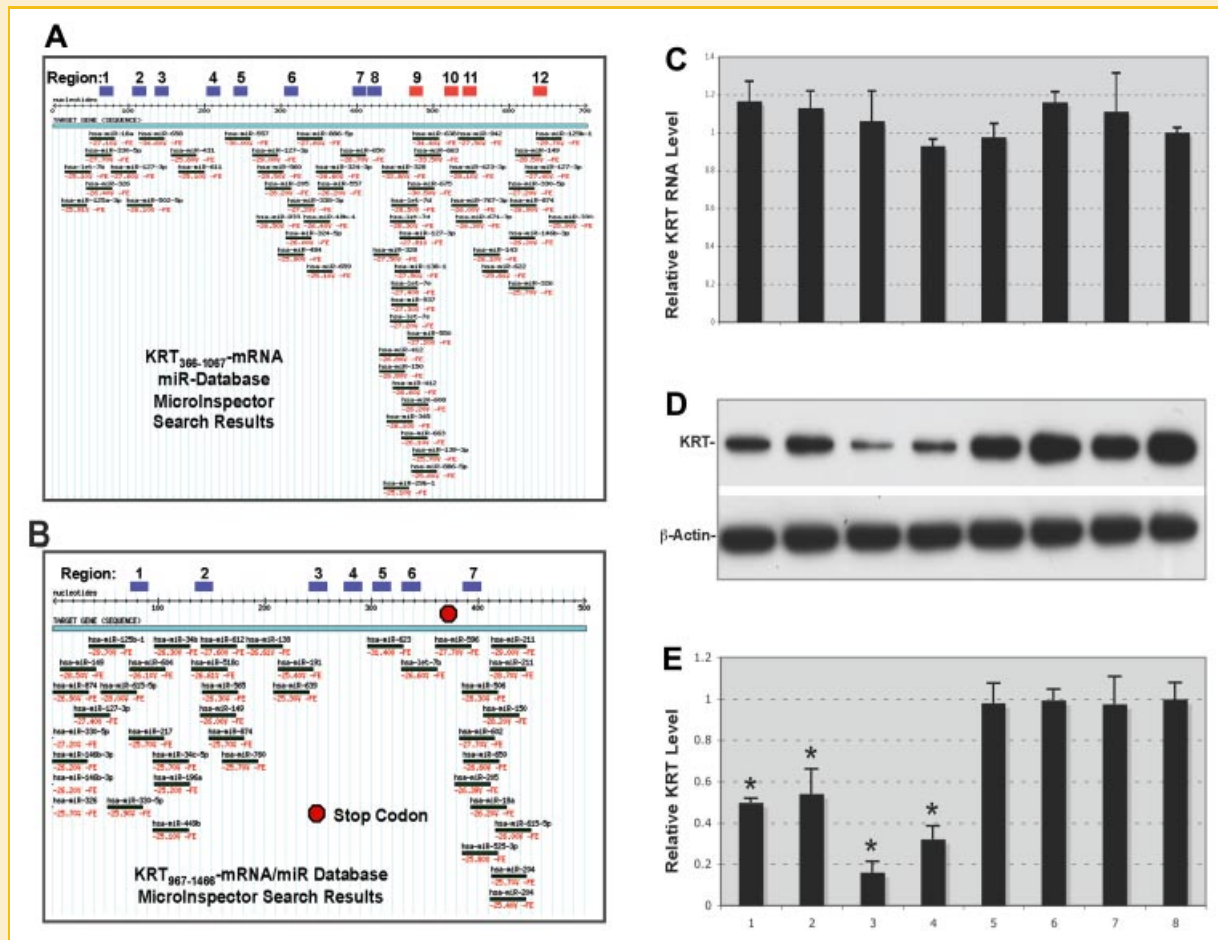


Fig. 2. MicroInspector alignment of miRs with KRT₃₆₆₋₁₀₆₇ and KRT₉₆₇₋₁₄₆₆ transcripts, and effects of miRs on cellular levels of KRT RNA and protein. Library selection was performed on the KRT segments as described, and the MicroInspector tool was then used to align miRs from the database with the respective segments of KRT. Results for KRT₃₆₆₋₁₀₆₇ are shown in panel A, and results for KRT₉₆₇₋₁₄₆₆ are shown in panel B. Library-selected regions are shown at the top of the panels; they are shown as 17 nt regions, based on the library size, although they may actually extend in either direction (for KRT₃₆₆₋₁₀₆₇, R1–R8, shown in blue, were identified on sequencing gels run for 1.5 h, and R9–R12, shown in red, were identified on gels run for 7.5 h). Eighty percent of the miRs which aligned with KRT₃₆₆₋₁₀₆₇ overlapped (≥ 5 nt) empirically identified accessible regions. The percentage of miRs which overlapped with accessible regions in KRT₉₆₇₋₁₄₆₆ was 76%, including the shift of regions 1 and 7 ($\Delta 1$ and $\Delta 7$ were shifted by six nucleotides) to compensate for RNase-H hydrolysis initiation. In particular, an astounding 17 aligned miRs overlapped with R9 in KRT₃₆₆₋₁₀₆₇ (panel A) and 7 aligned miRs overlapped with R7 which lies within the 3'-untranslated region of KRT₉₆₇₋₁₄₆₆ (panel B; the position of the stop codon is shown in red), with an additional 6 miRs aligned immediately 3' to R7. MCF7 cells were transfected with the specified miRs, and cells were harvested 48 h later. Panel C: RNA was examined for KRT transcripts using QPCR, with normalization to TBP (the amplicon was KRT₅₄₉₋₆₄₂). Additional controls included miRs which did not align with KRT. Panel D: KRT protein expression was examined by immunoblot analysis using an antibody against KRT. β -actin was used as a loading control. This shows results of a representative experiment. Panel E shows densitometric analysis of KRT protein expression levels from three independent experiments, as means \pm standard errors. Asterisk (*) indicates significant differences at $P < 0.01$ or greater from controls. For panels C–E: Lanes 1 and 2 show results with miRs which aligned with R1 (miR-125b-1 and miR-615-5p, respectively). Lane 3 shows results with an miR which aligned between R2 and R3 (miR-138). Lane 4 shows results with an miR which aligned with R6 (miR-let-7b). Lanes 5–7 show results with three miRs which aligned with R7 in the 3'-untranslated region (miR-205, miR-150, and miR-211, respectively). Lane 8 shows results with untreated MCF7 cells. Transfections without miR, or with a negative control miR which did not align with KRT were also without effect (data not shown; Lanes 5–7 effectively serve as negative controls for the protocol). Color figure can be viewed in the online issue, which is available at www.interscience.wiley.com.]

Immunoblot analyses for KRT protein (Fig. 2D,E) surprisingly showed that the three miRs which aligned with R7 within the 3'-UTR of KRT had no effect on KRT expression (Fig. 2). However, the miRs targeting R1 in the KRT₉₆₇₋₁₄₆₆ transcript produced significant reductions ($\sim 50\%$) in KRT protein expression (Fig. 2D,E). miR-138, which aligned with the KRT₉₆₇₋₁₄₆₆ transcript at a site lying between R2 and R3, had profound effects on KRT protein levels, with reductions of $\sim 85\%$ (ASOs to this region showed intermediate cleavage activity, $\sim 20\%$, in RNase-H-based assays). miR-let-7b,

which targeted R6 in the KRT₉₆₇₋₁₄₆₆ transcript, also produced substantial reductions ($\sim 70\%$) in KRT protein expression (Fig. 2). In this regard, miR-let-7b has recently been predicted to have a very high number (268!) of potential target genes [John et al., 2008]. We also tested three miRs which aligned with KRT₉₆₇₋₁₄₆₆, but which did so with lower match scores (-3438 ; specifically miR-let-7c*, miR-let-7f, and miR-let-7g). These produced smaller (but statistically significant) reductions in KRT protein ($\sim 40\%$; data not shown).

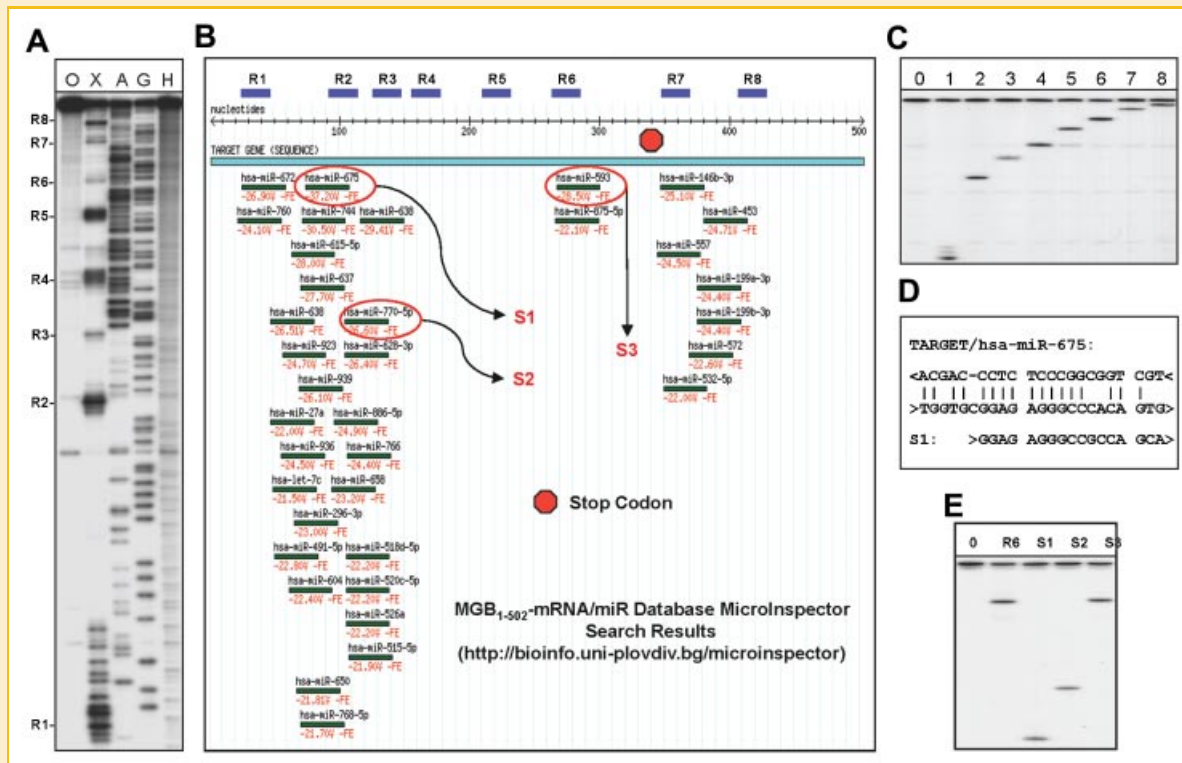


Fig. 3. MicroInspector-based alignment of miRs for the MGB₁₋₅₀₂ transcript and analysis of RNase-H-based cleavage. Using the web-based MicroInspector tool, the miR database was aligned to MGB₁₋₅₀₂ and compared with the N17-RNase-H-based library selection protocol (panel A shows library selection results, which identified eight accessible regions, designated as R1–8, indicated to the left). Lanes O, X, A, G, and H were as described in the legend of Figure 1. Panel B shows alignment results using the MicroInspector tool; library-selected regions R1–8 are shown in blue at the top. As is evident, most of the identified miRs (>80% of 36 miRs) overlapped (≥ 5 nt) the library-selected accessible sites. Also of interest is the fact that no miRs overlap R4 and especially R5 regions, so not all accessible regions are necessarily targeted. ASOs targeting the identified accessible sites all showed good activity in RNase-H-based assays (panel C). Three specific miRs (circled) targeting R2, R3, or R6 were selected based on their match scores, and 17mer ASOs were synthesized which matched a portion of the region the miRs targeted (designated as S1–3; panel B). Panel D shows the sequence and target alignment of ASO S1. The ASO corresponding to R6 identified by library selection was synthesized and tested using the RNase-H-based protocol, as were the S1–S3 ASOs (panel E). Results showed that all of the S1–S3 ASOs, which aligned with accessible sites in the target RNA, produced RNase-H-based cleavage equivalent to the library-selected R6 region. Randomly choosing ASOs not in library-selected sites nearly always results in little or no activity (data not shown). Color figure can be viewed in the online issue, which is available at www.interscience.wiley.com.]

Finally, given the surprisingly large number (17) of miRs which overlapped the R9 region in KRT₃₆₆₋₁₀₆₇, we arbitrarily selected three of these miRs for testing in transfection assays (miR-638, miR-675, and miR-127-3p). Curiously, none of these miRs had any effect on KRT mRNA (Fig. 4) or protein levels (KRT protein levels were $1.05 \pm 0.14\%$ of control levels), averaged over three independent experiments, with assays performed in triplicate.

Our data indicate that miRs with good complementarities to target RNAs overlap accessible sites in RNAs; about one-quarter of miRs aligned to regions not identified empirically in library selections, but these also were able to bind quite well to the RNA transcripts (based on RNase-H-based assays; not observing significant cleavage in random library selections could simply reflect a sensitivity issue). While it is not firmly established that susceptibility to RNase-H-mediated cleavage and/or binding of oligonucleotides indicates that such sites are necessarily accessible in vivo [Branch, 1998], a variety of studies support this contention [Milner et al., 1997; Southern et al., 1997; Duan et al., 2006; Kierzek et al., 2006]. In many

examples, accessible sites identified in vitro have been found to also be accessible in vivo [Milner et al., 1997; Southern et al., 1997; Pan et al., 2001]. Nevertheless, failure of the miRs aligning within the 3'-UTR of KRT, or within the R9 region, to inhibit translation could be due to protein masking of the sites in vivo.

None of the miRs identified by a computer-based alignment screen has previously been identified as targeting KRT. When arbitrarily selected aligned miRs were tested in transient transfection assays, many of the miRs which targeted areas within the coding region of KRT had profound/significant effects on KRT protein expression, while having no effect on KRT mRNA levels (by QPCR and Northern blot analyses). In contrast, three miRs which aligned to R7 in the 3'-untranslated region of KRT mRNA had no effect on KRT protein expression, even though ASOs targeting R7 functioned effectively in RNase-H-based assays. These results were somewhat surprising, since it is generally thought that miRs preferentially target sites in 3'-untranslated regions versus coding regions in mammals [John et al., 2008], although miRs do preferentially target coding regions in plants.

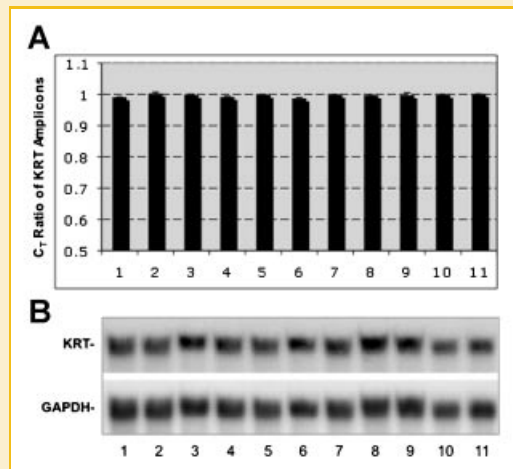


Fig. 4. Effects of miR transfection on KRT RNA levels. Assessment with multiple KRT amplicons and Northern blot analyses. Transfections were performed as described and 48 h following transfection, RNA was purified. Panel A: QPCR analyses were performed for a second amplicon in KRT, KRT_{1281–1381}. The results were analogous to those obtained with the KRT amplicon KRT_{548–648} (shown in Fig. 2). In addition to showing no change in KRT mRNA level, the ratios of the KRT_{1281–1381}/KRT_{548–648} amplicons were constant at unity in all samples (Y-axis), suggesting that KRT mRNA was intact and that no preferential degradation had occurred. Panel B: Northern blot analyses were also performed (in triplicate), which also showed no change in mRNA levels (vs. GAPDH as control). In additional transfection experiments, protein was harvested and examined by immunoblot analyses as described. Three independent experiments were performed, and analyses were run in triplicate. No change in KRT protein levels was observed in the three experimental miR transfections with miRs targeting region 9 in KRT (lanes 8–10), and the other samples showed changes similar to those previously reported (shown in Fig. 2). Lanes in panels A and B show: (1) miR-let-miR-7c^{*}; (2) miR-let-7f; (3) miR-let-7g; (4) miR-125b-1^{*}; (5) miR-615-5p; (6) miR-138; (7) miR-let-7b; (8) miR-638; (9) miR-675; (10) miR-127-3p; and (11) transfection control. A random miR was also without effect (not shown).

While it remains unclear how miR gene-regulatory networks have evolved, the observation that miRs can generally be aligned with accessible sites in target RNAs may indicate that their functional activities are enhanced by this property, a property which may also facilitate identification of miR targets.

ACKNOWLEDGMENTS

This work was supported in part by NIH/NCI IMAT grant CA118591 and funds from the Gittlen Cancer Research Foundation.

REFERENCES

Ambs S, Prueitt RL, Yi M, Hudson RS, Howe TM, Petrocca F, Wallace TM, Liu CG, Volinia S, Calin GA, Yfantis HG, Stephens RM, Croce CM. 2008. Genomic profiling of microRNA and messenger RNA reveals deregulated microRNA expression in prostate cancer. *Cancer Res* 68:6162–6170.

Bartel DP. 2004. MicroRNAs: Genomics, biogenesis, mechanism, and function. *Cell* 116:281–297.

Branch AD. 1998. Antisense drug discovery: Can cell-free screens speed the process? *Antisense Nucleic Acid Drug Dev* 8:249–254.

Bushati N, Cohen SM. 2007. microRNA functions. *Annu Rev Cell Dev Biol* 23:175–205.

Calin GA, Ferracin M, Cimmino A, di Leva G, Shimizu M, Wojcik SE, Iorio MV, Visone R, Sever NI, Fabbri M, Iuliano R, Palumbo T, Pichiorri F, Roldo C, Garzon R, Sevignani C, Rassenti L, Alder H, Volinia S, Liu CG, Kipps TJ, Negrini M, Croce CM. 2005. A microRNA signature associated with prognosis and progression in chronic lymphocytic leukemia. *N Engl J Med* 353:1793–1801.

Clawson GA, Bui V, Xin P, Wang N, Pan W. 2008. Intracellular localization of the tumor suppressor HtrA1/Prss11 and its association with HPV16 E6 and E7 proteins. *J Cell Biochem* 105:81–88.

Duan S, Mathews DH, Turner DH. 2006. Interpreting oligonucleotide microarray data to determine RNA secondary structure: Application to the 3' end of *Bombyx mori* R2 RNA. *Biochemistry* 45:9819–9832.

Esquela-Kerscher A, Slack FJ. 2006. Oncomirs—MicroRNAs with a role in cancer. *Nat Rev Cancer* 6:259–269.

Griffiths-Jones S, Saini HK, van Dongen S, Enright AJ. 2007. miRBase: Tools for microRNA genomics. *Nucleic Acids Res* 36:D154–D158.

Iorio MV, Ferracin M, Liu CG, Veronese A, Spizzo R, Sabbioni S, Magi E, Pedriali M, Fabbri M, Campiglio M, Menard S, Palazzo JP, Rosenberg A, Musiani P, Volinia S, Nenci I, Calin GA, Querzoli P, Negrini M, Croce CM. 2005. MicroRNA gene expression deregulation in human breast cancer. *Cancer Res* 65:7065–7070.

John B, Enright AJ, Aravin A, Tuschl T, Sander C, Marks DS. 2008. Human microRNA targets. *PLoS Biol* 6:e264.

Kierzek E, Kierzek R, Turner DH, Catrina IE. 2006. Facilitating RNA structure prediction with microarrays. *Biochemistry* 45:581–593.

Kluiver J, Kroesen BJ, Poppema S, Van den Berg A. 2006. The role of microRNAs in normal hematopoiesis and hematopoietic malignancies. *Leukemia* 20:1931–1936.

Lu J, Getz G, Miska EA. 2005. MicroRNA expression profiles classify human cancers. *Nature* 435:834–838.

Milner N, Mir KU, Southern EM. 1997. Selecting effective antisense reagents on combinatorial oligonucleotide arrays. *Nat Biotechnol* 15:537–541.

Nilsen TW. 2007. Mechanisms of microRNA-mediated gene regulation in animal cells. *Trends Genet* 23:243–249.

Pan WH, Clawson GA. 2004. Identification of efficient cleavage sites in long-target RNAs. *Methods Mol Biol* 252:125–144.

Pan WH, Clawson GA. 2006. Identifying accessible sites in RNA: The first step in designing antisense reagents. *Curr Med Chem* 13:3083–3103.

Pan W-H, Devlin H, Kelley C, Isom H, Clawson G. 2001. A selection system for identifying accessible sites in target RNAs. *RNA* 7:610–621.

Pan WH, Xin P, Bui V, Clawson G. 2003. Rapid identification of efficient target cleavage sites using a Hammerhead Ribozyme Library in an iterative manner. *Mol Therapy* 7:128–138.

Pan W, Xin P, Morrey J, Clawson G. 2004. A self-processing ribozyme cassette: Utility against human papillomavirus 11 E6/E7 mRNA and hepatitis B virus. *Mol Therapy* 9:596–606.

Rusinov V, Baev V, Minkov IN, Tabler M. 2005. MicroInspector: A web tool for detection of miRNA binding sites in an RNA sequence. *Nucleic Acids Res* 33:W696–W700.

Southern EM, Milner N, Mir KU. 1997. Discovering antisense reagents by hybridization of RNA to oligonucleotide arrays. *Ciba Found Symp* 209:38–46.

Volinia S, Calin GA, Liu CG, Ambs S, Cimmino A, Petrocca F, Visone R, Iorio M, Roldo C, Ferracin M, Prueitt RL, Yanaihara N, Lanza G, Scarpa A, Vecchione A, Negrin M, Harris CC, Croce CM. 2006. A microRNA expression signature of human solid tumors defines cancer gene targets. *Proc Natl Acad Sci USA* 103:2257–2261.

Wu L, Belasco JG. 2008. Let me count the ways: Mechanisms of gene regulation by miRNAs and siRNAs. *Mol Cell* 29:1–7.

Zhang B, Pan X, Cobb GP, Anderson TA. 2007. microRNAs as oncogenes and tumor suppressors. *Dev Biol* 302:1–12.